

# **EFFECTS OF THE LOW EMISSIVITY SHIELDS ON PERFORMANCE AND POWER USE OF A REFRIGERATED DISPLAY CASE**



*Southern California Edison  
Refrigeration Technology and Test Center  
Energy Efficiency Division*

*August 8, 1997*



## DISCLAIMER

THIS WORK (**WORK**) WAS PERFORMED WITH REASONABLE CARE AND IN ACCORDANCE WITH PROFESSIONAL STANDARDS. HOWEVER, NEITHER **SCE** NOR ANY ENTITY PERFORMING THE **WORK** PURSUANT TO **SCE'S** AUTHORITY MAKE ANY WARRANTY OR REPRESENTATION, EXPRESSED OR IMPLIED, WITH REGARD TO THIS REPORT, THE MERCHANDABILITY OR FITNESS FOR A PARTICULAR PURPOSE OF THE RESULTS OF THE **WORK**, OR ANY ANALYSES, OR CONCLUSIONS CONTAINED IN THIS REPORT.

THE RESULTS REFLECTED IN THE **WORK** ARE BASED GENERALLY REPRESENTATIVE OF OPERATING CONDITIONS; HOWEVER, THE RESULTS IN ANY OTHER SITUATION MAY VARY DEPENDING UPON PARTICULAR OPERATING CONDITIONS.

## TABLE OF CONTENTS

Executive Summary.....	ii
List of Tables .....	iv
List of Figures .....	iv
Appendix Contents.....	vi
Nomenclature.....	vii
Introduction.....	1
Display Case Heat Transfer Modes .....	2
Shield Description .....	4
Test Facility.....	6
RTTC's Test Equipment .....	7
Test Procedure.....	13
Data Acquisition Procedure.....	14
Analysis .....	15
Data Collection/Reduction .....	15
Screening Procedure.....	16
Calculations .....	16
Discussion of Results .....	22

## EXECUTIVE SUMMARY

The purpose of this project was to test and evaluate the impact of the low emissivity aluminum shields on the power use and thermal performance of a multi-deck display case, commonly used in supermarkets for storing and refrigerating dairy products. This display case was tested in a controlled environment maintained at 75 °F and 50% relative humidity, and served by a refrigeration system using a Hydrofluorocarbon (HFC) refrigerant, R-404A.

Thermal radiation and convection of warm air into the cold display case accounts for most of its refrigeration load. Aluminum shields can be utilized to cover the front opening of the display case and reduce the radiative and convective heat transfer into the case, thereby reducing the power use while improving the product temperature maintenance.

Supermarkets operate on a narrow profit margin and refrigeration is their largest energy end-use. Any reduction in refrigeration load could lower their energy cost and improve their competitiveness. Furthermore, increasing their products shelf lives could enhance their profit margin. As a result, testing and verifying the impact of these shields on the display cases could be advantageous to Edison supermarket customers.

Southern California Edison (SCE) conducted this test at its state-of-the-art Refrigeration Technology and Test Center (RTTC), located in Irwindale, CA. The RTTC's sophisticated instrumentation and data acquisition system provided detailed tracking of the refrigeration system's critical temperature and pressure points during the test period. These readings were then utilized to quantify various heat transfer and power related parameters within the refrigeration cycle. The results of SCE's test focused on three typical scenarios found mostly in supermarkets:

Scenario -1 (no shields - base case)	Non 24 hour operation with no shields utilized during closing hours (from midnight to 6:00 A.M.)
Scenario -2 (shields applied)	Non 24 hour operation with shields applied during closing hours (from midnight to 6:00 A.M.) and fully opened for the remaining 18 hours
Scenario -3 (holiday)	Shields applied for a full 24 hour period

Test results indicate that applying shields will reduce the refrigeration load and the power consumption of the compressor. Additionally, the product temperature will stay at lower levels with shields closed for about 15 hours after they were opened. Obviously, the effects of shields on the compressor power and refrigeration load was reduced under scenario 2, which in reality, is a common situation for utilizing such shields. During off-cycle defrost, it was observed that shields increased the coil ice melting period. The summary table depicts the impact of these low emissivity shields on various refrigeration parameters.

Summary Table

Scenario	Discharge Air Temperature (°F)	Average Product Temperature (°F)	Refrigeration Load of the Case* (MBtu/hr-ft)	Compressor Power (kW)	Rating* (kW/Ton)
(1) - Base Case	35.6	40.6	1.6	3.1	1.16
(2) - Non-24-hour Supermarket with Shields	34.4	38.9	1.4	2.9	1.23
% Δ	3.3%	4.0%	12.6%	9.0%	-5.6%
(3) - Holiday Case	32.2	36.1	1.0	2.0	1.27
% Δ	9.7%	11.0%	41.0%	36.0%	-9.0%

\* Calculated Values

## LIST OF TABLES

Summary Table .....		iii
Table 1 - Effects of Utilizing Heat Reflecting Shields on Refrigeration System Parameters for a Non-24-hour Supermarket with Shields and Holiday Case versus Base Case .....		2
Table 2 - List of Sensors Used.....		12
Table 3 - Testing Conditions and Scenarios for Shield Test.....		14
Table 4 - Calculated Results (for the Base Case Scenario) .....		21

## LIST OF FIGURES

Figure 1 - Effects of Utilizing Heat Reflecting Shields on Refrigeration System Parameters for a Non-24-hour Supermarket with Shields and Holiday Case versus Base Case .....		2
Figure 2 - Display Case with Shields Closed.....		4
Figure 3 - RTTC Floor Plan.....		6
Figure 4 - RTTC Piping and Instrumentation .....		7
Figure 5 - Location of Sensors within the Display Case.....		15
Figure 6 - Product Temperature Variation Chart .....		22
 Key Parameters Over Time		
Figure 7a - Base Case.....		23
Figure 7b - Non-24-hour Supermarket with Shields Case .....		23
Figure 7c - Holiday Case.....		24
Figure 8 - Average Product Temperature Comparison Between Base Case, Non-24-hour Supermarket with Shields Case, and Holiday Case.....		24

Key Parameters Profiles for Sample 24-hour Periods

Figure 9a - Starting with Shields Open, then Closing them During the  
Second Defrost Period .....25  
Figure 9b - Starting with Shields Closed, then Opening them During the  
Second Defrost Period .....25

Mass Flow Rate and Compressor Power Profiles for Sample 24-hour Periods

Figure 10a - Starting with Shields Open, then Closing them During the  
Second Defrost Period .....26  
Figure 10b - Starting with Shields Closed, then Opening them During the  
Second Defrost Period .....26  
Figure 11 - Refrigeration Effect and Refrigeration Load per Foot versus Time .....27  
Figure 12 - Average Discharge Air Temperature Comparison Between Base Case,  
Non-24-hour Supermarket with Shields Case, and Holiday Case .....28

Last Defrost Period of the Day

Figure 13a - After Shields were Closed.....28  
Figure 13b - After Shields were Opened.....29

## NOMENCLATURE

$T_{db}$	Room dry bulb temperature (°F)
$T_{dp}$	Room dew point temperature (°F)
RH	Relative Humidity of the room (Taken from the Trane Psychrometric Chart based on the average dry bulb and dew point temperatures) (%)
$DAT_1$	Discharge air temperature @ location (1) (°F)
$DAT_2$	Discharge air temperature @ location (2) (°F)
$DAT_3$	Discharge air temperature @ location (3) (°F)
$DAT_{avg}$	Average discharge air temperature (°F)
MAT	Mid air curtain temperature (°F)
RAT	Return air temperature (°F)
ACTD	Temperature Drop across the Air Curtain (°F)
$PT_{top}$	Product temperature @ top shelf (°F)
$PT_{bottom}$	Product temperature @ bottom shelf (°F)
$PT_{avg}$	Average product temperature (°F)
$T_{air_e}$	Air temperature entering evaporator (°F)
$T_{air_L}$	Air temperature leaving evaporator (°F)
$\Delta T_{air}$	Temperature difference of air across evaporator (°F)
$T_{evap_1}$	Evaporator temperature @ location (1) (°F)
$T_{evap_2}$	Evaporator temperature @ location (2) (°F)
$T_{evap_3}$	Evaporator temperature @ location (3) (°F)
$T_{evap_{avg}}$	Average evaporator temperature (°F)
$TD_{approx}$	Temperature Difference between entering air and evaporator temperature (°F)
MFR	Mass flow rate of refrigerant (lb/min)
$ST_1$	Suction temperature of refrigerant @ location 1 (°F)
$ST_2$	Suction temperature of refrigerant @ location 2 (°F)
$ST_3$	Suction temperature of refrigerant @ location 3 (°F)
$ST_{avg}$	Average suction temperature of refrigerant (°F)
SP	Suction pressure of refrigerant (psig)
SDP	Saturated discharge pressure of refrigerant (psig)
CR	Compression ratio of compressor
$T_{cond_{in}}$	Temperature of superheated refrigerant vapor entering condenser (°F)
$H_{cond_{in}}$	Enthalpy of superheated refrigerant vapor entering condenser (Btu/lb)
$T_{cond_{exit}}$	Temperature of liquid refrigerant leaving condenser (°F)
$H_{cond_{exit}}$	Enthalpy of liquid refrigerant leaving condenser (Btu/lb)
$T_{evap_{exit1}}$	Temperature of superheated refrigerant vapor leaving evaporator @ location 1 (°F)
$T_{evap_{exit2}}$	Temperature of superheated refrigerant vapor leaving evaporator @ location 2 (°F)
$T_{evap_{exit3}}$	Temperature of superheated refrigerant vapor leaving evaporator @ location 3 (°F)
$T_{evap_{exitavg}}$	Average temperature of superheated refrigerant vapor leaving evaporator (°F)
SSP	Saturated Suction Pressure (psig)
SST	Saturated suction temperature (°F)
$He_{vap_{exit}}$	Enthalpy of superheated refrigerant vapor leaving evaporator (Btu/lb)

$H_{comp_{in}}$	Enthalpy of superheated refrigerant vapor entering compressor (Btu/lb)
$T_{subcool_1}$	Subcooled temperature of liquid refrigerant entering expansion valve @ location 1 (°F)
$T_{subcool_2}$	Subcooled temperature of liquid refrigerant entering expansion valve @ location 2 (°F)
$T_{subcool_3}$	Subcooled temperature of liquid refrigerant entering expansion valve @ location 3 (°F)
$T_{subcool_{avg}}$	Average subcooled temperature of liquid refrigerant entering expansion valve (°F)
$H_{satliq}$	Calculated value of enthalpy at saturated temperature corresponding to saturated discharge pressure (Btu/lb)
$T_{sat_{SDP}}$	Temperature of saturated liquid @ discharge pressure (°F)
$\Delta T_{subcool}$	Temperature difference between subcooled liquid entering the expansion valve and saturated liquid leaving the condenser (°F)
$C_{p_{subcool}}$	Specific heat of subcooled liquid refrigerant entering expansion valve (Btu/lb °F)
$\Delta H_{subcool}$	Enthalpy change between subcooled liquid entering expansion valve and saturated liquid leaving condenser (Btu/lb)
$H_{subcool}$	Calculated value of enthalpy of subcooled refrigerant entering expansion valve (Btu/lb)
$T_{postexp}$	Temperature of refrigerant in the mixed phase leaving expansion valve (°F)
$W_{comp}$	Actual work input of the compressor (kW)

# 1 INTRODUCTION

The purpose of this test was to evaluate the impact of low emissivity aluminum shields on the power use and thermal performance of a multi-deck display case typically used in supermarkets for storing dairy products. Southern California Edison (Edison) conducted this test at its state-of-the-art Refrigeration Technology and Test Center (RTTC), located in Irwindale, California. The RTTC's sophisticated instrumentation and data acquisition system provided detailed tracking of the refrigeration system's critical temperature and pressure points during the test. These readings were then utilized to quantify various heat transfer and power related parameters of the refrigeration cycle.

Supermarkets operate on a narrow profit margin. Energy costs play a crucial role in supermarket economics and competitiveness. In many cases, the annual energy costs for a supermarket equals or exceeds the sales profit. A supermarket's annual energy costs depend heavily on the refrigeration systems' energy use. Thermal radiation and convection of warm air into the cold display case accounts for most of its refrigeration load. Aluminum shields can be utilized to cover the front opening of the display case and reduce the radiative and convective heat transfer into the case, thereby reducing the power use while improving the product temperature maintenance. Any reduction in refrigeration load could lower a supermarket's energy cost and improve its competitiveness. Furthermore, increasing their products' shelf life could enhance their profit margin. As a result, testing and verifying the impact of these low emissivity shields on the display cases could be advantageous to Edison's supermarket customers.

A large number of the supermarkets in the Edison service territory are closed to the public for approximately six hours at night. This time could be used to reduce the overall energy consumption of the refrigeration cases by enclosing the cases with heat reflective shields. Based on this fact, Edison's test focused on three typical scenarios found mostly in supermarkets:

Scenario -1 (no shields - base case)	Non-24 hour operation with no shields utilized during closing hours (from midnight to 6:00 A.M.)
Scenario -2 (shields applied)	Non-24 hour operation with shields applied during closing hours (from midnight to 6:00 A.M.) and fully opened for the remaining 18 hours
Scenario -3 (holiday)	Shields applied for a full 24-hour period

The base case for this test considered the daily operating hours of a supermarket where shields were not utilized during closing hours. In scenario 2, shields were utilized for the six hours during which the store is closed to the public (12 midnight to 6 A.M.). The holiday case (scenario 3) assumed a full 24-hour period with the shields closed to simulate the effects of a supermarket possibly being closed for a holiday.

The results of Edison's test indicate that using heat reflecting shields during the six hours that a supermarket is closed may decrease the power consumption and cooling load of the dairy cases by 9 percent and 12.6 percent, respectively. Equipping existing equipment with these shields, will allow the

display case discharge air temperature to be lowered by about 1 °F (from 35.6 °F to 34.4 °F), while the mass flow rate will be lowered by 12.1 percent. Table 1 and Figure 1 summarize the effects of utilizing heat reflecting shields on various parameters of the refrigeration system.

The heat rejection to the condenser was reduced by 11.9 percent, potentially allowing for a smaller condenser cost in new construction projects.

Table 1 - Effects of utilizing Heat Reflecting Shields on Refrigeration System Parameters  
Non-24-hour Supermarket with Shields and Holiday Case versus Base Case

Scenario	Discharge Air Temp. (°F)	Average Saturated Suction Temp. (°F)	Average Product Temp. (°F)	Mass Flow Rate of Refrigerant (lb/min)	Refrigeration Load of the Case* (MBtu/hr-ft)	Condenser Heat Rejection* (MBtu/hr)	Compressor Power (kW)	Rating* (kW/Ton)
(1) - Base Case	35.6	19.0	40.6	9.5	1.6	41.9	3.1	1.16
(2) - Non-24-hour Supermarket with Shields	34.4	19.0	38.9	8.4	1.4	36.9	2.9	1.23
% Δ	3.3%	0.0%	4.0%	12.1%	12.6%	11.9%	9.0%	-5.6%
(3) - Holiday Case	32.2	18.6	36.1	5.7	1.0	25.7	2.0	1.27
% Δ	9.7%	2.4%	11.0%	40.3%	41.0%	38.7%	36.0%	-9.0%

\*Calculated Values

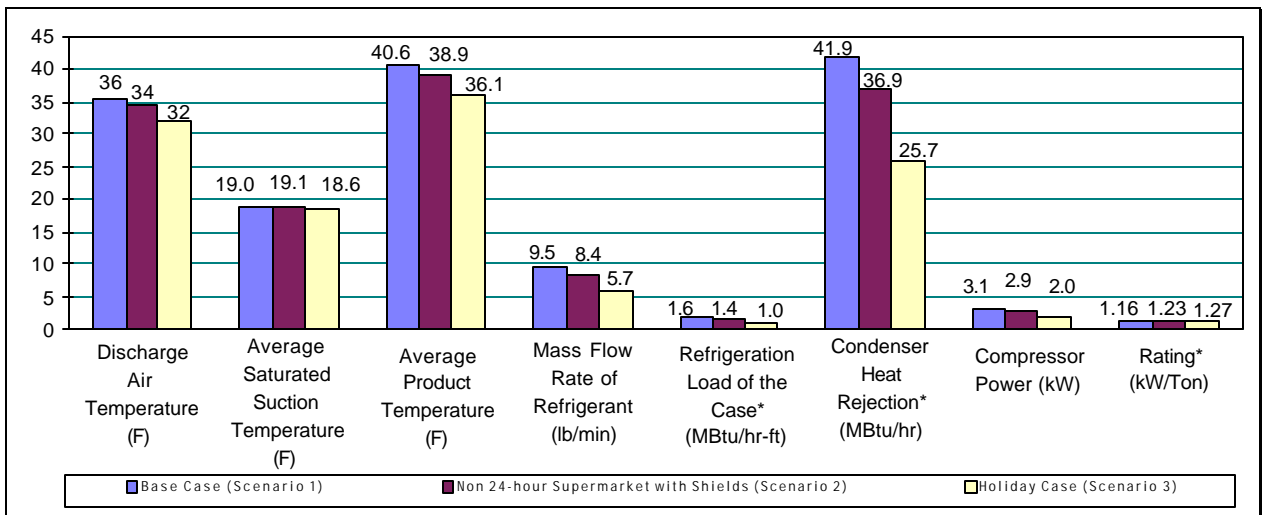


Figure 1 - Effects of utilizing Heat Reflecting Shields on Refrigeration System Parameters  
Non-24-hour Supermarket with Shields and Holiday Case versus Base Case

## DISPLAY CASE HEAT TRANSFER MODES

Heat transfer components of the display case include infiltration (convection), transmission (conduction), and radiation. The following sections discuss these modes of heat transfer in detail.

## Infiltration Load

Heat transfer through the air curtains, also known as infiltration, functions as a convective load. The air curtain in open display cases acts as a primary barrier to reduce the infiltration load. The total performance of the air curtain and the quantity of heat transferred across it depends on several factors, including:

- Air jet's velocity and temperature
- Number of jets
- Air jet width
- Surrounding's temperature and humidity ratio
- Rate of traffic adjacent to the air curtain
- Display case temperature and humidity ratio

An air curtain consists of a stream of air discharged from a series of small nozzles within a honeycombed configuration at the top of the display case. The air is discharged downward toward a return grill located approximately two feet above the floor on the front panel of the case. The air is drawn into a circulating fan where it picks up the fan motor heat and passes through the cooling coil (or the evaporator). By flowing across the evaporator, the air loses its sensible and latent heat. The chilled air is then returned to the discharge grill. The discharged air passes adjacent to the still air in the store and within the case. The still air mixes with the discharged air and this mixed stream develops new thermal characteristics. The mixing or entrainment takes place regardless of the store and display case temperatures. The temperature gradient between the cold display case and warm surroundings within the mixing (or entrained) zone causes the sensible heat from the warm side to transfer into the cold side. Furthermore, during the entrainment process, the air curtain absorbs moisture from the store which will eventually act as a latent load. The infiltration total sensible and latent loads can be expressed by:

$$Q_{inf} = cfm_{entrained} \cdot 4.5 \cdot \Delta h$$

where

$Q_{inf}$	=	Infiltration load, Btu/hr
$cfm_{entrained}$	=	Entrained air flow into the case as a result of mixing, ft <sup>3</sup> /min
$\Delta h$	=	Difference between the enthalpy of the store air and the display case air, Btu/lb

## Transmission Load ( $Q_T$ )

Transmission load is a function of the case wall thermal conductivity, interior and exterior air film conductance, and the temperature difference between the interior and the exterior of the case. In a general simplified form, the following equation can represent this load.

$$Q_T = U \cdot A \cdot \Delta T$$

where

$Q_T$	=	Transmission load, Btu/hr
$U$	=	Overall heat transfer coefficient, Btu/hr- °F-ft <sup>2</sup>
$A$	=	Exterior surface area of the display Case, ft <sup>2</sup>
$\Delta T$	=	Difference between display case temperature and the surrounding air temperature, °F

### Radiation Load ( $Q_R$ )

The heat gain of the display case through radiation is a function of the case inside conditions including wall temperature, wall emissivity, wall area, and view factor with respect to the surrounding (store) walls/objects, floor, ceiling, and their corresponding emissivities and areas. In a simplified approach, with respect to two gray surfaces, this quantity can be given by:

$$Q_R := \frac{\sigma \cdot (T_{oR}^4 - T_{iR}^4)}{\left\{ \frac{1 - \epsilon_{CS}}{\epsilon_{CS} \cdot A_{CS}} \right\} + \frac{1}{A_S \cdot F} + \frac{1 - \epsilon_S}{\epsilon_S \cdot A_S}}$$

where

$Q_R$	=	Radiation load, Btu/hr
$\sigma$	=	Stefan-Boltzmann constant, Btu/hr-ft <sup>2</sup> -°F <sup>4</sup>
$T_{oR}$	=	Room temperature, °F
$T_{iR}$	=	Case internal surface temperature, °F
$\epsilon_{CS}$	=	Case surface emissivity
$\epsilon_S$	=	Room surfaces representational emissivity
$A_{CS}$	=	Surface area of the display case, ft <sup>2</sup>
$F$	=	View factor between the case and surroundings

### SHIELD DESCRIPTION

Utilizing shields (Figure 2) is expected to reduce the radiation and infiltration loads of a display case. Additionally, it is expected to maintain lower product temperatures, thereby improving the products' shelf life.



Figure 2 - Display Case with Shields Closed

The choice of aluminum as a shield material as opposed to other materials readily available is due to its low emissivity. Materials with a low emissivity, such as aluminum, absorb very little radiated heat from the environment and reflect most of the heat back to the surroundings. The following equation, using a simplified case of radiation, expresses the relationship between reflectivity and emissivity in general:

$$\epsilon = 1 - \rho$$

where

$$\begin{aligned} \epsilon &= \text{Emissivity} \\ \rho &= \text{Reflectivity} \end{aligned}$$

In addition, all shields act as air infiltration barriers reducing the convection of warm air into the air curtain and decreasing the return air temperature. Consequently, these shields may reduce the evaporator sensible and latent loads. Other shield materials with higher emissivities tend to absorb more radiation heat, and eventually transfer that heat into the case via conduction. The radiation heat absorbed by the shield is given by:

$$Q_{\text{Rshield}} = \sigma \cdot A \cdot \epsilon \cdot F \cdot (T_{\text{room}}^4 - T_{\text{shield}}^4)$$

where

$$\begin{aligned} Q_{\text{Rshield}} &= \text{Radiation load on the shield, Btu/hr} \\ \sigma &= \text{Stefan-Boltzmann constant, Btu/hr-ft}^2\text{-}^\circ\text{F}^4 \\ A &= \text{Surface area of the shield, ft}^2 \\ \epsilon &= \text{Emissivity of the shield} \\ F &= \text{View factor between the shield and the room} \\ T_{\text{room}} &= \text{Room temperature, }^\circ\text{F} \\ T_{\text{shield}} &= \text{Shield exterior surface temperature, }^\circ\text{F} \end{aligned}$$

This test utilized a woven aluminum fabric, coated with a thin transparent film to eliminate oxidation and provide strength. A vertical rolling curtain arrangement, permanently attached to the top of the display case, was the other feature of the shield.

Differences in temperature and humidity between the inside of the display case and the ambient environment often cause condensation to form between the inner and outer fabric surfaces of the shields. Prevention of condensation on the aluminum fabric used in the test was provided via a precise pattern of tiny holes. The holes allowed the shields to breathe and condensed moisture to evaporate.

## TEST FACILITY

Edison's RTTC includes a refrigeration room, a controlled environment room and a computer room (Figure 3). The center is equipped with the state-of-the-art refrigeration test and data acquisition systems. Figure 4 illustrates the piping and major equipment used at the RTTC. This unique facility can test the performance of various refrigerants under actual supermarket indoor conditions. These tests can evaluate the performance of refrigerants with respect to numerous key parameters, including varying condensing and suction temperatures. Moreover, RTTC can assess the impact of numerous commercial refrigeration retrofit technologies on the performance of most defined systems.

The controlled environment room contains the low and medium temperature display cases, while the refrigeration room houses the sophisticated refrigeration and chiller test racks. The computer room houses the computer terminals loaded with sophisticated software which facilitates data recording and the programming of various modes of operation of the refrigeration rack.

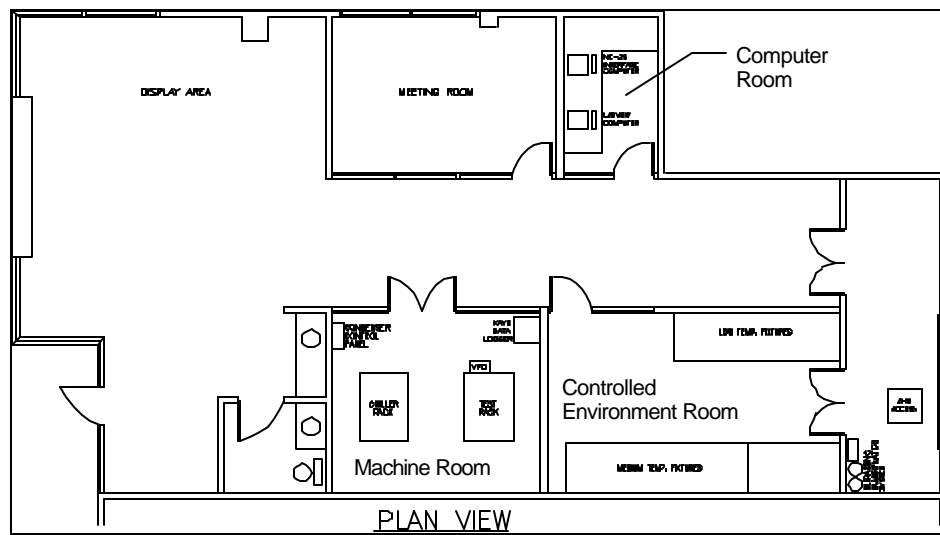


Figure 3 - RTTC Floor Plan

The controlled environment is an isolated thermal zone served by independent heating, cooling and humidification systems. The sensible cooling load representing people and other heat gain sources is provided by a constant volume direct expansion system reclaiming the waste refrigeration heat via a six row coil. While the air is conditioned to a desired thermostatic set point, an advanced ultrasonic humidification unit introduces precise moisture amounts to the air surrounding the display cases, representing the latent load due to outside air and people.

The refrigeration test rack, with the aid of a separate chiller system, can operate under various condensing temperatures. Additionally, the refrigeration system can be served by four individual heat rejection devices. The RTTC is capable of evaluating the performance of refrigeration systems under the most defined loads, utilizing air-cooled, evaporatively-cooled, and water-cooled condensers.

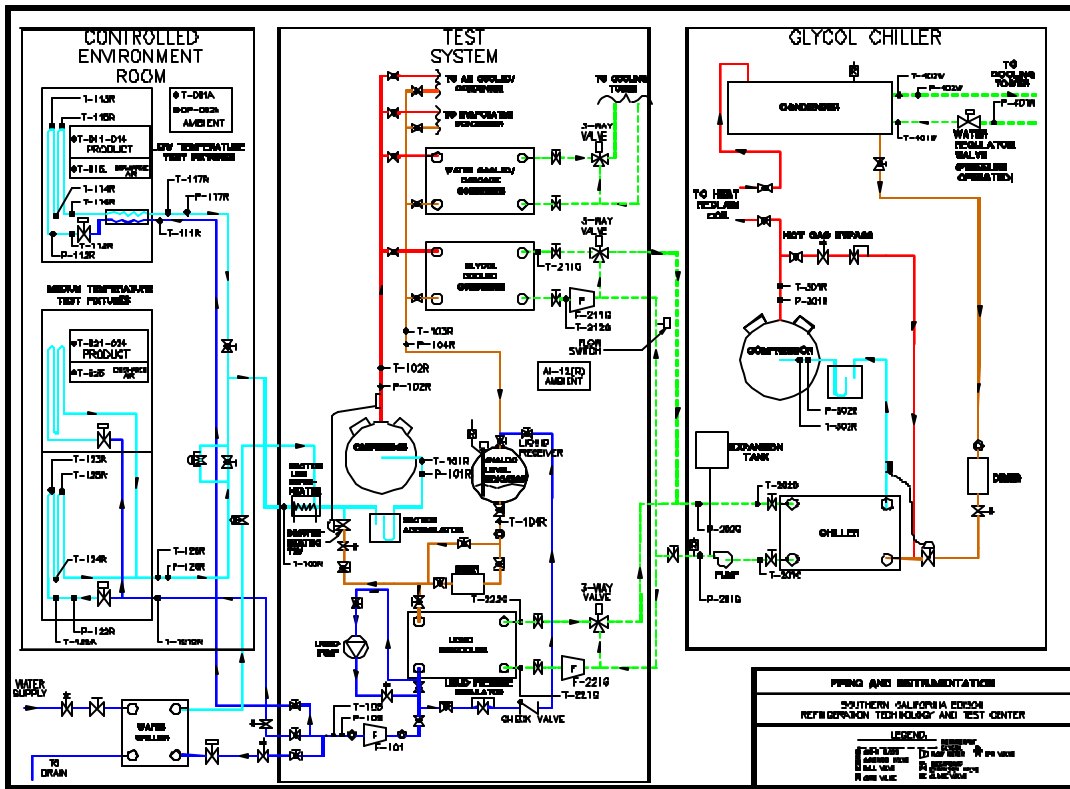


Figure 4 - RTTC Piping and Instrumentation

## RTTC'S TEST EQUIPMENT

### Refrigeration Test Rack

1. Major Components:
  - a. Compressor:
    - 1 - Carlyle 6.5 HP, four cylinder, Model 06DR820 semi-hermetic compressor
  - b. Condenser:
    - 1 - Alfa-Laval brazed plate-type condenser:
 

Heat Rate: 59,000 BTU/Hr

Flow Rate: 870 Lb./Hr. R-12; 13 GPM glycol
  - c. Receiver Tank:
 

Standard Refrigeration, P/N UV-70, 10" diameter X 28" high vertical receiver tank.

- d. Subcooler:
  - 1 - Alfa-Laval plate-type subcooler:
    - Heat Rate: 12,400 BTU/Hr
    - Flow Rate: 870 Lb./Hr. R-12; 5 GPM glycol
- 2. Auxiliary Components:
  - a. Suction Accumulator
  - b. Suction Filter
  - c. Crankcase Heater
  - d. Oil Fail Switch, electronic type
  - e. Suction De-superheating Expansion Valve
  - f. Liquid Pump, Smith Precision Products Model GC-1, equipped with a Smith Precision Products Model WW-120 Liquid Bypass Differential Regulator.
  - g. Danfoss YLT-3011 Variable Speed Drive for test compressor

### **Chiller Rack**

- 1. Major Components:
  - a. Compressor:
    - 1 - Carlyle 6.5 HP, four cylinder, Model 06DR820 semi-hermetic compressor.
  - b. Condenser:
    - 1 - Standard Refrigeration shell and tube condenser, Model # SST755-8 Pass.
  - c. Chiller:
    - 1 - Alfa-Laval brazed plate-type chiller:
      - Heat Rate: 66,900 BTU/Hr
      - Flow Rate: 977 Lb./Hr. R-22; 15 GPM glycol

### **Control System**

The control system for the project's refrigeration equipment is as follows:

Danfoss NC-25 microprocessor-based control system, with analog input, analog output and digital I/O boards

### **Auxiliary Components**

Three heating cables were provided for simulation of a long return suction line: Heating cables are tightly attached to the suction line with gear type clamps. The suction line and heaters are insulated with 2" fiberglass insulation with PVC jacket.

### **Medium Temperature Display Fixture**

Cases, Tyler DDCM8 and DDCM12 - 4 rows of shelving, 20" wide.

Lights, 800 mA fluorescent, one row in the canopy.

Defrost Type: Ambient

This case is equipped with standard thermostatic expansion valves and LSHX

### **Low Temperature Display Fixture**

Cases, Tyler D6F124 - 4 rows of shelving, 22" wide.

Lights, 430 mA fluorescent, two rows in the canopy and one row nose light.

Defrost Type: Electric

This case is equipped with thermostatic expansion valves and LSHX

### **HVAC Equipment for Controlled Environment Area**

1. Air Handler, one Magic Aire Model 36 BH air handler (without coil)  
Motor: 3/4 HP, 2-speed  
Air Flow Rate at External static Pressure: 1500 cfm @ 0.75 in-wg
2. Humidifier, one type-ENS Stulz Ultrasonic humidifier. The humidifier is installed inside the air stream of the distribution ductwork downstream of the heat reclaim coil.
3. Heat Reclaim Coil:  
Heat of Rejection: 89,950 BTU/Hr (available)

### **Major Data Acquisition System Components**

1. Data Scanner, Kaye Instruments Digi-4 Model #X1520S. Kaye's Digi-4 has a special emphasis on temperature measurement, with excellent thermocouple signal processing. The scanner was calibrated at the factory, and is traceable to NIST standards.  
Analog inputs:
  - a. Fifty-six special grade, type-T thermocouple inputs ( $\pm 0.03^{\circ}\text{C}$ )
  - b. Fifteen precision 100  $\Omega$  Platinum Resistance Temperature Device (RTD) inputs ( $\pm 0.01^{\circ}\text{C}$ )
  - c. Twenty-three analog inputs from pressure and other various transducers.

### Outputs:

- a. RS-232 Communication link, one report every ten seconds. (A report includes instantaneous values of all data points)
2. User Interface, IBM compatible 80486-based PC, running National Instruments' LabView 3.0 for Windows. A communications link was maintained with the data-scanning equipment at all times. The PC also provided the system with data storage and remote (modem) data access to the projects' test data.

In general, the PC provided the following functions:

- a. Communicated continuously with the data scanner (via RS-232), acquiring one full data record (all scanned inputs) every ten seconds. The data was then averaged over a two-minute period, and the two-minute averages written to storage (hard disk).
- b. Maintained modem communication capability (for contact by a remote computer) and when requested, transmitted user specified files to the remote system.
- c. Provided graphical representation of system performance data, both real-time and historical. Real-time graphic displays consisted of: 1) a schematic representation of the system, with the flows, temperatures, pressures, and other process data indicated on the screen, and 2) trend graph windows. The data to be displayed in the trend graph windows was user-configurable, with up to 18 variables in three separate graph windows.

### Measurement Point Configuration

#### 1. Refrigerant and Water/Glycol Line Precision Temperature Points

A single 100  $\Omega$  Platinum RTD is located in a thermo-well installed in the appropriate line. Two high-accuracy type-T thermocouples located on opposing sides of the line within one or two inches of the RTD thermo-well. The thermocouples provide a confidence check on the RTD measurement, and are firmly mounted to the outside of the bare refrigeration line using a heat transfer compound.

#### 2. Case Discharge Air and Controlled Environment Area Ambient Temperatures

A single 100  $\Omega$  Platinum RTD is located in free air. Two high-accuracy type-T thermocouples located within one or two inches of the RTD. The thermocouples provide a confidence check on the RTD measurement.

#### 3. Pressure Measurements

Pressure Transducers are fitted to 1/8" NPT female side connections located on dedicated transducer valves.

#### 4. Refrigerant Mass Flow

The refrigerant mass flow meter is a coriolis effect device, installed in the refrigerant liquid line.

#### 5. Water/Glycol Flow meters

The water/glycol flow meters are turbine-type sensors.

#### 6. kW (Power)

The measurements were taken by factory calibrated CT-transducer combinations, which provided analog outputs. The instantaneous power measurements were integrated with respect to time, yielding kWh, and the kW measurements were taken in five places:

- Input of the variable speed drive device
- Input to the compressor motor
- Input to the condenser fan-motor
- Input to the display-case fan-motor
- Input to the display-case lighting

#### 7. Dew Point Sensor

The dew point sensor utilizes chilled-mirror technology.

#### 8. Informational Temperature Points

These points are located at various points in the refrigeration and water/glycol circuits. These consist of a single, high-accuracy type-T thermocouple, mounted to the bare copper line using a heat transfer compound.

Informational temperatures are also located in the display fixtures. High-accuracy, type-T thermocouples are located at various locations in each display fixture, on the coils and in the product containers, and at the mid-point of the air curtain.

Table 2 - List of Sensors Used

Sensor Type	Make / Model	Accuracy [NIST Traceable]
Dew Point	EG&G DewTrak Model 200	$\pm 1^\circ \text{F}$
Refrigerant Mass Flow	Micro Motion Model DS065S	$\pm 0.2\%$
Power (kW1)	Ohio Semitronics Model PC5-062BX680	$\pm 0.5\% \text{ F.S. } (.04 \text{ kW})$
Power (kW2)	Ohio Semitronics Model P-143B	$\pm 1.0\% \text{ F.S. } (.08 \text{ kW})$
Power (kW3)	Ohio Semitronics Model PC5-062BX680	$\pm 0.5\% \text{ F.S. } (.04 \text{ kW})$
Power (kW4)	Ohio Semitronics Model PC5-062BX680	$\pm 0.5\% \text{ F.S. } (.04 \text{ kW})$
Power (kW5)	Ohio Semitronics Model PC5-062BX680	$\pm 0.5\% \text{ F.S. } (.04 \text{ kW})$
Water/Glycol Flow	EG&G Flow Technology Model FT8-8NENW-LEG-1	$\pm 1\%$
Pressure	Setra Transducers Model 207 - 100 & 500 PSIG Pressure Ranges	$\pm 0.13\%$
Temperature (RTD)	Hy-Cal Engineering Model RTS-37-A-100	$\pm 0.01^\circ \text{C}$
Temperature (T/C)	Kaye Instruments T/W 50 through 80; Melt # 8032	$\pm 0.1^\circ \text{C}$

## TEST PROCEDURE

The shelves of the Tyler medium temperature dairy case were stocked with plastic gallon containers of water in an arrangement typically found in supermarkets. Water was used to represent milk due to its reasonably close specific heat capacity. Sixty-minute time initiated, time-terminated defrosts at six hour intervals were used in accordance with Tyler's recommendations to provide defrost for the cases. Supermarket shopper traffic was simulated by the use of an intermittently oscillating fan.

Space conditions were maintained in the controlled environment by a constant volume air handler. A six-row coil connected to the chiller rack reclaimed the heat of refrigeration and provided the sensible heating to the space. To maintain humidity in the space, an ultrasonic humidifier, installed in the supply air duct downstream of the heat reclaim coil, injected moisture into the air stream. Motorized bypass dampers adjusted the flow of air through the heat reclaim coil to obtain the precise supply air temperature required. The conditions within the controlled environment room were held constant at  $75 \pm 0.3$  °F and 50 percent relative humidity.

Temperature measurements considered to be critical to the process were recorded from a group of three sensors (one RTD and two thermocouples). These data points were extracted from the daily files, and the readings from the thermocouples were compared to each other, and to the reading from the associated RTD. The difference between sensor readings was compared to criteria established during the commissioning of the data acquisition system. Any data where the maximum difference fell outside the allowable standard deviation was flagged for further review.

The operation of the compressor, condenser, display case, and HVAC system were controlled by the microprocessor controller. The microprocessor controller was equipped with a stand-alone modem for remote access to the control parameters. An interface with the microprocessor controller was made through a serial connection to a PC located in the computer room. Through this interface all parameters of microprocessor control could be modified and inspected.

The Variable Frequency Drive (VFD) modulated the compressor speed (and thereby its capacity and the refrigerant mass flow rate) according to inputs from the microprocessor controller. The microprocessor controller changed the VFD output to the compressor according to *differences between actual and target case discharge air temperature and suction pressure*.

An evaporator pressure regulator (EPR) valve was utilized downstream from the evaporator to maintain a fixed pressure at the evaporator and prevent the coil temperature from falling below a minimum set point. Without the EPR valve, the evaporator coil could essentially freeze when the shields are utilized because of the lower return air temperatures.

Heating control for the controlled environment room was accomplished with motorized dampers at the air handler that modulated to adjust the amount of airflow through the heat reclaim coil. Separately, the ultrasonic humidifier varied the amount of water vapor released into the air stream according to inputs from the microprocessor controller. The microprocessor controller adjusted the magnitude of change for the heating and humidification of the space according to differences between the target and actual dry bulb temperatures and relative humidity, respectively.

Tests were conducted over six twenty-four hour periods under various conditions (table 3). The first day of the test, April 29<sup>th</sup>, the display case was initially open with no shields present in order to establish the base case steady-state conditions. The test was run with this configuration until 9:00 A.M. on April 30<sup>th</sup>, and then the shields were closed. The closed shield scenario continued until 9:00 A.M. on May 2<sup>nd</sup>, at which time the shields were opened. The remainder of the test was run with the shields open to return to steady-state conditions. Throughout the test, the saturated condensing temperature was maintained at a fixed value of 89.5 °F.

Table 3 - Testing Conditions and Scenarios for Shield Test

April 29 <sup>th</sup>	April 30 <sup>th</sup>	May 1 <sup>st</sup>	May 2 <sup>nd</sup>	May 3 <sup>rd</sup>	May 4 <sup>th</sup>
Shields open 100% . Established steady-state conditions	Shields open until 2 <sup>nd</sup> defrost period, at which time shields were closed 100%.	Shields closed 100%.	Shields closed until 2 <sup>nd</sup> defrost period, at which time shields were opened 100%	Shields open 100%.	Shields open 100%. Verification of steady-state conditions.

## DATA ACQUISITION PROCEDURE

With the objective of minimizing instrument error and maintaining a high level of repeatability and accuracy in the data and careful attention was paid to the system design. To obtain this goal, the following steps were taken:

1. Use of sensors with the highest accuracy available.
2. Minimization of sensor drift errors by use of redundant sensors.
3. Utilization of calibration standard instruments of the highest accuracy.
4. Elimination of interference from power conductors and high frequency signals by double-shielding sensor leads.

A Kaye Instruments Digi-4 Model #X1520S Data Scanner was used to log the data. Kaye’s Digi-4 has a special emphasis on temperature measurement, with excellent thermocouple signal processing. The data scanner processes 94 data channels. The scanner was calibrated at the factory, and is traceable to NIST standards. The system has 56 special grade type-T thermocouples accurate to  $\pm 0.03^{\circ}\text{C}$ , 15 precision 100 $\Omega$  platinum Resistance Temperature Device (RTD) inputs accurate to  $\pm 0.01^{\circ}\text{C}$ , and a combination of 23 analog inputs from pressure transducers, dew point sensors, flow meters, and CT-transducers. An RS-232 communication link sent one data report that included instantaneous values of all data points every ten seconds. To ensure that the data collection was not compromised by the control sequence’s priority over data acquisition, the data acquisition system for the project was designed to be completely independent of the supervisory control computer.

Every 10 seconds the data acquisition system sampled the entire 94 point data array and created time-stamped two-minute averages. The two-minute data was then saved to a file which was closed at the end of each 24-hour period. Every 24 hours, the data collected from the previous 24 hours was downloaded remotely for screening and processing.

The raw data, as well as environmental conditions in the controlled room, were analyzed daily for consistency and accuracy. In the event that any of the test parameters fell outside acceptable limits, the problem was flagged. In such cases, test runs were repeated upon correction of the problem.

## ANALYSIS

### Data Collection/Reduction

The test facility is equipped with a sophisticated data acquisition system that scans 94 sensors and logs their outputs on two-minute intervals. Data was collected and stored for each sensor for six days. Every 24 hours during the test, the data was downloaded and checked for consistency and accuracy. Operating parameters were checked and deemed to be within acceptable limits before the next run was started. Figure 5 depicts the locations of various sensors within the display case.

The collected data points from the two-minute intervals were averaged into one-hour blocks for each 24-hour period. After the hourly data was developed, the calculation tables were created.

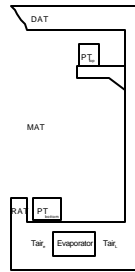


Figure 5 - Location of Sensors within Display Case

The base case scenario was comprised of data from May 3<sup>rd</sup>, the first full day after the shields were re-opened and the data reached steady-state conditions. The holiday scenario utilized data from May 1<sup>st</sup>, the first full 24-hour day with shields closed.

The selection of the data for scenario 2 was done to represent a typical 24-hour period for a supermarket which utilizes shields during its closing hours. The typical non 24-hour operational supermarket scenario was composed of data from the following testing times. The effects of utilizing the shield were best shown by using 6 hours of closed shield data (the first six hours of May 1<sup>st</sup>), followed by 16 hours of open display case data (10 hours after the shields were re-opened on May 1<sup>st</sup>, as well as 6 hours of May 2<sup>nd</sup>).

## Screening Procedure

Once the data was compiled into hourly averages within the spreadsheet, tabular and graphical representations of various correlations and calculated parameters were produced. Several graphs were created to initially screen the data. The initial screening plots are located in Appendix. Included in this group were the fundamental data points provided by the data acquisition system. These plots were used to determine the validity of each test. After careful examination of the initial screening plots, the informational plots were produced. This set provided relationships that are of interest to the supermarket customers. The two-minute data was also analyzed for this test. With more data points to analyze, the trends in the data were more easily determined by using the two-minute data as opposed to the hourly data.

## Calculations

A series of calculations were performed to obtain the key refrigeration parameters including refrigeration effect, refrigeration load of the case, heat rejection at the condenser, heat of compression, and compressor power per ton.

After the data was downloaded from the data logger and the data of interest was extracted, some preliminary calculations were performed. These calculations included averaging temperature data that were read by more than one sensor. Such data included discharge air temperature, product temperature, temperature at the evaporator inlet, saturated suction temperature, temperature at the evaporator exit, and temperature of refrigerant entering the expansion valve.

The refrigeration load of the case, heat rejection at the condenser, and compressor power per ton, all depend on the refrigerant available, heat, or enthalpies at different locations of the refrigeration cycle. Enthalpies can be either obtained from the refrigerant manufacturer's data at various temperatures and pressures, or calculated with respect to specific heat capacities and temperatures.

Once the temperatures and pressures were determined, the enthalpies were obtained. DuPont's Suva Refrigerant Expert Program, version 2.0 was used to determine the enthalpies of superheated vapor. The data logger provided all pressures in gage unit, and after conversion to absolute, the Refrigerant Expert was used to look up the enthalpies. The Refrigerant Expert program was used to obtain enthalpies at the evaporator exit, and the compressor and condenser inlets.

The enthalpies in the saturated phase were calculated using temperature-dependent expressions provided by DuPont, as well as using basic thermodynamic relationships. Equation 1, provided by DuPont, determined the enthalpy in kJ/kg of refrigerant 404A for a temperature range of -20 °C to 40 °C. The temperatures of the saturated liquid were first converted to Celsius, then inserted into equation 1 to produce the corresponding saturated enthalpy. The enthalpy at the condenser exit and the enthalpy at saturated temperature and discharge pressure were found by use of the equations 1 and 2.

$$1) \quad H = A + BT + CT^2$$

H = Enthalpy (kJ/kg)

A = 200

B = 1.438333  
 C = 0.003916667  
 T = Temperature (°C)

where A, B, and C were constants determined by DuPont from the relationship between saturated enthalpy and temperature. Next, equation 2 was used to convert the enthalpy in kJ/kg to Btu/lb. Because of a change in reference states from SI to English units, a reference conversion, H (ref), was included in Equation 2.

$$2) \quad H \text{ (Btu/lb)} = [H \text{ (kJ/kg)} - H \text{ (ref)}] \cdot 0.43021 \text{ (Btu/lb / kJ/kg)}$$

H (ref) = 145.6 kJ/kg for R404A

The Refrigerant Expert program does not provide subcooled enthalpies, therefore, in order to find the enthalpies for subcooled refrigerant, the thermodynamic relationship between enthalpy and temperature was incorporated. For this relationship, however, the correct liquid specific heat capacity was needed. Equation 3, provided by DuPont, calculated the liquid specific heat capacity of refrigerant 404A for a temperature range of -40 °F to 140 °F. The enthalpy at the entrance to the expansion valve was found using this equation and subcooled temperature.

$$3) \quad C_p = 0.306 + 4.083E-4 T - 1.194E-6 T^2 + 8.056E-8 T^3$$

C<sub>p</sub> = Liquid Heat Capacity (Btu/lb °F).

T = Average temperature of the subcooled liquid (°F) for a range of -40 °F to 140 °F

The temperature difference between the subcooled liquid entering the expansion valve and the saturated liquid leaving the condenser was needed in order to find the corresponding enthalpy change due to subcooling.

$$4) \quad \Delta T_{\text{subcool}} = T_{\text{sat}} - T_{\text{subcool}_{\text{avg}}}$$

$\Delta T_{\text{subcool}}$  = Temperature difference between subcooled liquid entering the expansion valve and saturated liquid leaving the condenser (°F).

$T_{\text{subcool}_{\text{avg}}}$  = Average pre-expansion valve temperatures (°F). This value was read directly using the data acquisition system.

$T_{\text{sat}}$  = Temperature of Saturated Liquid at Saturated Discharge Pressure (°F). This value was determined by look-up using DuPont's Suva Refrigeration Expert Program and saturated discharge pressure data from the data acquisition system.

Next, the enthalpy change between the subcooled and saturated liquid was calculated by utilizing the following thermodynamic relationship.

$$5) \quad \Delta H_{\text{subcool}} = C_p \cdot \Delta T_{\text{subcool}}$$

Finally, the enthalpy of the subcooled liquid was computed. In order to accomplish this, the enthalpy change between the subcooled and saturated liquid was subtracted from the enthalpy of saturated liquid.

$$6) \quad H_{\text{subcool}} = H_{\text{satliq}} - \Delta H_{\text{subcool}}$$

$\Delta H_{\text{subcool}}$  = Enthalpy change between subcooled liquid entering the expansion valve and saturated liquid leaving the condenser (Btu/lb).

$H_{\text{subcool}}$  = The subcooled liquid enthalpy entering the expansion valve (Btu/lb).

$H_{\text{satliq}}$  = Saturated liquid enthalpy (Btu/lb). This value was determined using equations 1 and 2.

After determination of all enthalpy values, calculations were made to determine parameters of interest such as refrigeration effect, refrigeration load of the case, heat of compression, heat rejection at the condenser, sensible load of the evaporator, compressor power per ton, and coefficient of performance.

Refrigeration effect is the quantity of heat that each unit mass of refrigerant absorbs to cool the refrigerated space. It simply represents the capacity of the evaporator per pound of refrigerant. It was calculated by subtracting the enthalpy of subcooled liquid entering the expansion valve from the enthalpy of superheated refrigerant at the evaporator exit (equation 7). Because the refrigeration effect is directly proportional to the saturation suction temperature, it is affected by changes in product temperature or discharge air temperature settings, and therefore saturated suction temperature.

$$7) \quad RE = H_{\text{evap}_{\text{exit}}} - H_{\text{subcool}}$$

RE = Refrigeration Effect (Btu/lb)

$H_{\text{evap}_{\text{exit}}}$  = Enthalpy of superheated refrigerant vapor at the evaporator exit (Btu/lb).

The refrigeration load of the case is the amount of cooling or heat removal that takes place at the evaporator of the display case per hour (equation 8). This value is inversely proportional to saturation suction temperature, and is thus affected by changes in product temperature or discharge air temperature settings.

$$8) \quad Q_{\text{case}} = \text{mfr} \cdot k \cdot RE$$

$Q_{\text{case}}$  = Refrigeration Load of the case (Btu/hr)

mfr = Mass flow rate of refrigerant (lb/min)

k = Conversion Factor, 60 (min/hr)

Typically, the refrigeration load of the case is expressed on a per linear foot basis. Therefore, the refrigeration load per foot of the case was calculated by dividing the refrigeration load of the case by 20 feet, the length of the test case (equation 9).

$$9) \quad Q_{\text{case/ft}} = Q_{\text{case}} / 20\text{ft}$$

$Q_{\text{case/ft}}$  = Refrigeration Load per foot of the case (Btu/ft-hr)

It is also important to determine the refrigeration load of the case in tons. Thus, the refrigeration load of the case was divided by 12,000, a conversion factor from Btu/hr to tons (equation 10).

$$10) \quad Q_{\text{case}} (\text{tons}) = Q_{\text{case}} / 12000$$

$Q_{\text{case}} (\text{tons}) = \text{Refrigeration Load of the case (tons)}$

Obtaining the heat of compression is also of interest because it can be used to calculate the amount of heat rejection at the condenser and the theoretical compressor power necessary to provide cooling for the system. Because the heat of compression is the difference between the enthalpies at the suction and discharge sides of the compressor, this value is also affected by variations in suction temperature (equation 11). The saturated condensing temperature remained unchanged at 89.5 °F throughout the test. Therefore, the superheated, high pressure enthalpy of the refrigerant vapor at the condenser inlet was used instead of the refrigerant enthalpy at the compressor discharge to obtain the heat of compression.

$$11) \quad Q_{\text{comp}} = \text{mfr} \cdot k \cdot (H_{\text{cond}_{\text{in}}} - H_{\text{comp}_{\text{in}}})$$

$Q_{\text{comp}}$  = Heat of Compression (Btu/hr)

$k$  = Conversion Factor, 60 (min/hr)

$H_{\text{cond}_{\text{in}}}$  = Enthalpy at the inlet to the condenser (value determined by look-up using DuPont's Suva Refrigeration Expert Program)

$H_{\text{comp}_{\text{in}}}$  = Enthalpy at the inlet to the compressor (value determined by look-up using DuPont's Suva Refrigeration Expert Program)

The heat rejection at the condenser was calculated based on the total heat of the system. The total heat of the system is a function of the sum of the heat removal rate at the evaporator and the heat of compression. The total heat rejected at the condenser can also be obtained by the product of mass flow rate and change in refrigerant enthalpies between the inlet and outlet of the condenser which includes de-superheating, latent (or phase change), and subcooling heat removals within the condenser.

The analysis, however, evaluated the heat rejection based on the enthalpies at the condenser inlet and saturated liquid (equation 12). This approach yielded results less than one percent difference versus the total heat of the system (heat removal at the evaporator plus heat of compression).

$$12) \quad Q_{\text{cond}} = \text{mfr} \cdot k \cdot (H_{\text{cond}_{\text{in}}} - H_{\text{satliq}})$$

$Q_{\text{cond}}$  = Heat Rejection at the Condenser (Btu/hr)

$k$  = Conversion Factor, 60 (min/hr)

The sensible load of the evaporator is the amount of cooling the evaporator provides to reduce the air temperature without removing any of its moisture content. It was calculated by utilizing equation 13.

$$13) \quad Q_{\text{senscoil}} = \text{CFM} \cdot \rho_{\text{air}} \cdot C_{p_{\text{air}}} \cdot k \cdot \Delta T_{\text{air}}$$

$Q_{\text{senscoil}}$  = Sensible load of the evaporator (Btu/hr)

- CFM = Volume flow rate of air (ft<sup>3</sup>/min)
- $\rho_{\text{air}}$  = 0.0749 lb/ft<sup>3</sup>
- $C_{p_{\text{air}}}$  = 0.24 Btu/lb °F
- k = Conversion Factor, 60 (min/hr)
- $\Delta T_{\text{air}}$  = Air temperature drop across the evaporator (°F)

To calculate the volume flow rate of air across the evaporator, the cross sectional area of the discharge air grill was multiplied by the velocity of the air across the coil (equation 13a).

$$13a) \quad \text{CFM} = V \cdot A$$

V = Velocity of air (ft/min). This value was assumed based on various manufacturer's data.

A = Cross Sectional Area (ft<sup>2</sup>)

The cross sectional area of the air discharge grill is a product of the width of the air discharge grill and the length of the refrigeration case (equation 13b).

$$13b) \quad A = L \cdot W$$

L = Length of Refrigeration Case (ft)

W = Width of air discharge grill (ft)

The coefficient of performance is a dimensionless ratio that determines the efficiency of the system. It is the relationship between how much cooling the system provides (refrigeration load of the case, Btu/hr) and how much power the system uses (compressor power, Btu/hr) (equation 14). Consequently, the larger the coefficient of performance, the more efficient the cycle performs.

$$14) \quad \text{COP} = Q_{\text{case}}/Q_{\text{comp}}$$

COP = Coefficient of performance

The evaporator coil cools the air, and the cooled air in turn removes the heat gained by the display case. In cooling the air, the evaporator sensibly cools the air, and as a result, air temperature drops. It also provides latent cooling of the air which dehumidifies the air, and thereby lowers its moisture content. The sensible heat ratio is a characteristic index for the coil and is the ratio of sensible cooling to total cooling (sensible and latent) of the evaporator coil (equation 15). It indicates how well the coil removes air moisture.

$$15) \quad \text{SHR} = Q_{\text{senscoil}}/Q_{\text{case}}$$

SHR = Sensible Heat Ratio

Table 4 provides a summarized version (of calculated results) for the base case scenario. The blue rows indicate the defrost periods which were ignored in the analysis. During defrosts, to make heat available to the heat rejection coil, a false load was imposed on the refrigeration system. During these periods, the liquid line was routed into a plate heat exchanger to remove the false load of city water passing through the heat exchanger. Hence, defrost values (shown in the blue rows) are not relevant to the test.

Table 4 - Calculated Results (for the Base Case Scenario)

Hour	RE (Btu/lb)	Qcase (Btu/hr)	Qcase/ft (Btu/hr ft)	Qcase (Tons)	Qcomp (Btu/hr)	Qcond (Btu/hr)	Qsenscoil (Btu/hr)	MFR/ton (lb/min-ton)	COP	Eff <sub>actual</sub> (kW/ton)	SHR
1	55.7	31449	1572	2.62	9648	41437	13963	3.59	3.26	1.14	0.44
2	55.9	31797	1590	2.65	9776	41845	13811	3.58	3.25	1.16	0.43
3	55.9	32429	1621	2.70	9981	42659	13931	3.58	3.25	1.13	0.43
4	73.4	42679	2134	3.56	7510	40838	3698	2.73	5.68	1.13	0.09
5	57.9	37640	1882	3.14	11045	47917	11946	3.46	3.41	1.11	0.32
6	55.8	32686	1634	2.72	10020	43032	13651	3.58	3.26	1.14	0.42
7	55.9	32034	1602	2.67	9818	42066	13777	3.58	3.26	1.14	0.43
8	55.8	32094	1605	2.67	9878	42222	13746	3.58	3.25	1.14	0.43
9	56.0	31986	1599	2.67	9829	41962	13866	3.57	3.25	1.14	0.43
10	64.7	36995	1850	3.08	7644	40485	4100	3.09	4.84	1.21	0.11
11	57.0	37991	1900	3.17	11389	49150	11832	3.51	3.34	1.09	0.31
12	55.9	33516	1676	2.79	10330	44115	13614	3.58	3.24	1.11	0.41
13	55.8	32765	1638	2.73	10128	43257	13902	3.59	3.24	1.12	0.42
14	55.8	32356	1618	2.70	10010	42706	13812	3.59	3.23	1.13	0.43
15	55.9	31688	1584	2.64	9802	41769	13898	3.58	3.23	1.15	0.44
16	71.6	42582	2129	3.55	7878	41907	5792	2.79	5.40	1.10	0.14
17	57.7	38488	1924	3.21	11339	49168	11980	3.47	3.39	1.08	0.31
18	56.0	32983	1649	2.75	10175	43475	13529	3.57	3.24	1.14	0.41
19	55.9	32078	1604	2.67	9908	42282	13475	3.58	3.24	1.14	0.42
20	55.8	32425	1621	2.70	10025	42784	13613	3.58	3.23	1.12	0.42
21	55.9	32435	1622	2.70	10159	42891	13628	3.58	3.19	1.13	0.42
22	73.1	41542	2077	3.46	7490	40048	4617	2.74	5.55	1.12	0.11
23	59.5	37338	1867	3.11	10431	46021	10854	3.36	3.58	1.13	0.29
24	55.9	33575	1679	2.80	10322	44177	13375	3.58	3.25	1.11	0.40
Daily Avg.	58.7	34731	1737	2.89	9772	43259	11850	3.43	3.63	1.13	0.35
Std. Dev.	5.74	3666	183	0.31	1081	2467	3447	0.29	0.81	0.03	0.12

## DISCUSSION OF RESULTS

Reversal of product temperature distribution as a result of shields application was one of the first observations in this test. With an open display case, entrainment of the warm test-room's air (at 75 °F) into the cold case and the mixing effect that takes place within the air curtain plane, can increase the temperature of products near the return air grill, as well as the return air temperature. Whereas utilizing the shields, it was observed that products located on the bottom shelf were approximately 2 °F cooler than those on the top shelf (Figure 6). However, without the shields, the products located on the top shelf were slightly colder than those on the bottom shelf. Also, the bottom shelf was about 5 °F cooler with the shields down than it was with the shields up. With little or no air infiltration from the outside, the cold air from the case settles at the bottom of the case due to the density gradients formed by the different air temperatures. This accounts for the cold temperatures at the bottom shelves.

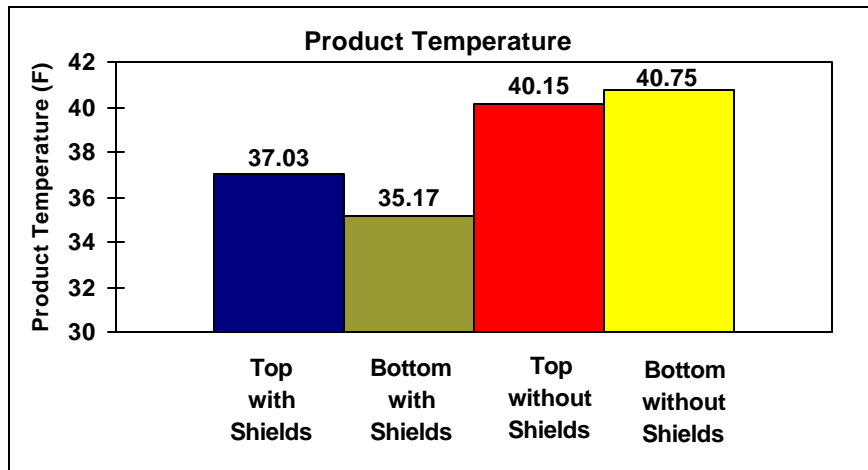


Figure 6 - Product Temperature Variation

It was also observed that during the first hour after defrost termination, the evaporator coil sensible heat-ratio dropped by about 29 and 27 percent, with and without shields, respectively. This reduction in the sensible heat ratio indicated a larger quantity of latent load was imposed on the coil due to moisture migration from the room to the case when the system was in defrost.

By utilizing the shield arrangement, the rate of heat gain to the case due to radiation and infiltration decreased. The shield assembly during the non-24-hour supermarket with shields and holiday scenarios caused the refrigeration load of the case to decrease by 12.6 and 41.0 percent, respectively (Figures 7a through 7c). Also, the compressor power decreased by 0.2 kW and 1.1 kW for the non-24-hour supermarket with shields and holiday scenarios, respectively. Obviously, utilizing shields for extended hours of operation provides the most reduction in refrigeration load and power use. The discharge air temperature was lower than the base case by 1.2 °F and 3.4 °F for the same scenarios. The effect of the evaporator pressure regulator valve in maintaining a minimum saturated suction temperature caused the

evaporator temperature to remain almost constant between approximately 22 °F and 24 °F throughout the three test scenarios.

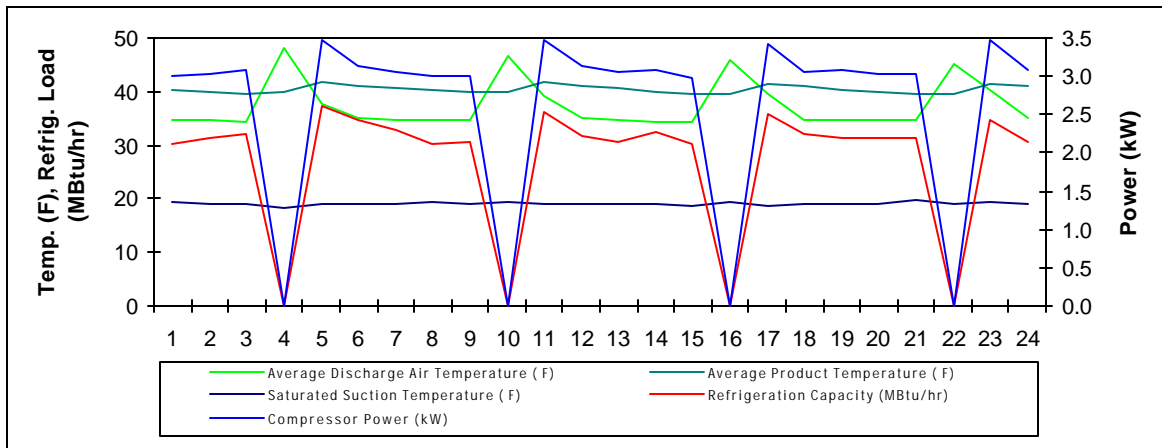


Figure 7a - Key Parameters over Time for Base Case

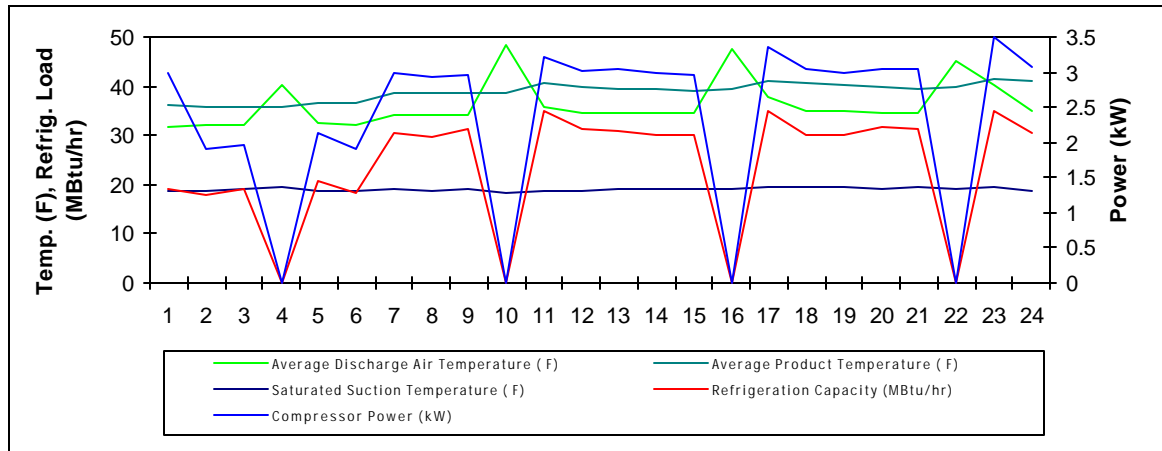


Figure 7b - Key Parameters over Time for Non-24-hour Supermarket with Shields Case

The compressor kW decreased as a result of the decreased case load. Less refrigerant mass flow was required to satisfy the target saturated suction pressure and discharge air temperature control setting.

The effectiveness of the discharge air stream to hold and reduce product temperature increased with the case shields down. The difference in the average daily product temperatures between shields up and shields down was 3 °F for the upper and 5 °F for the lower products. Correspondingly, the temperature difference for the average discharge air temperature from the base case was 1.2 °F and 3.4 °F for the non-24-hour supermarket with shields and holiday scenarios, respectively.

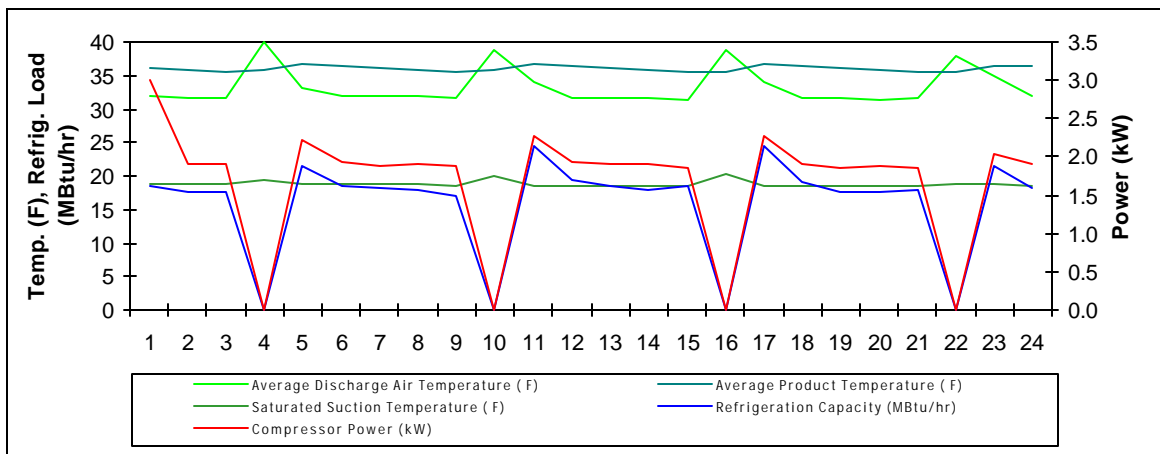


Figure 7c - Key Parameters over Time for Holiday Case

The difference in average product temperature created by utilizing the shields was the largest in the holiday case, and had only a modest impact in the non-24-hour supermarket with shields case. The base case and holiday case consistently differed by approximately 4 °F throughout the 24-hour period (Figure 8). On the other hand, the temperature difference between base case and non-24-hour supermarket with shields case started at approximately 4 °F (same as holiday case), but after the shields were opened, the difference lessened until their temperatures became equal (at approximately 9 P.M.). Utilizing the shields for six hours allowed the product temperature to remain below that of base case for 15 hours after the shields were removed. This could result in less overall compressor energy requirement to maintain lower product temperatures.

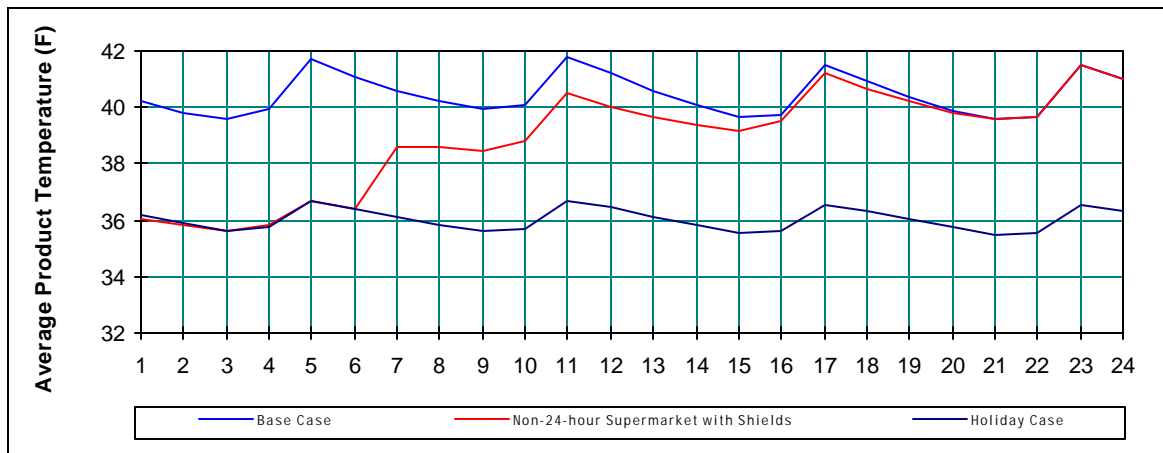


Figure 8 - Average Product Temperature Comparison Between Base Case, Non-24-hour Supermarket with Shields Case, and Holiday Case

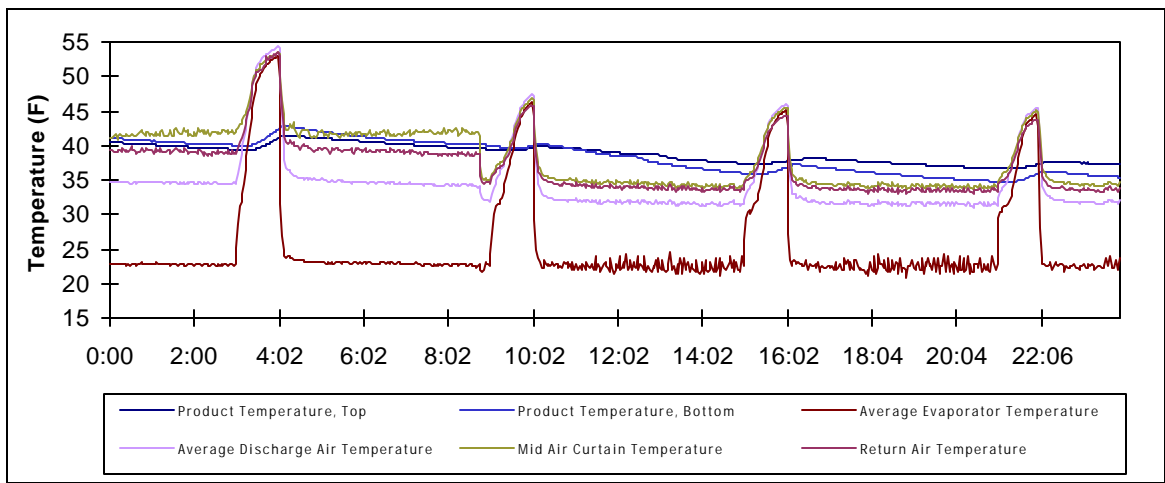


Figure 9a - Key Parameters Profile for a sample 24-hour period starting with shields open, then closing them during the second defrost period

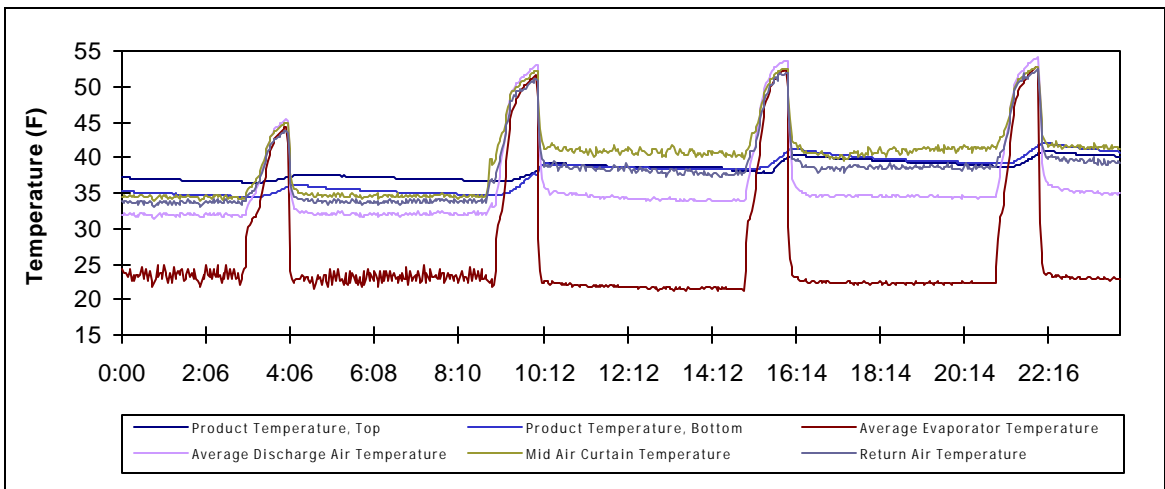


Figure 9b - Key Parameters Profile for a sample 24-hour period starting with shields closed, then opening them during the second defrost period

Figures 9a, 9b, 10a, and 10b present the transitional effects of shields on the key refrigeration parameters for two sample test days. The first day (Figure 9a), the shields were open initially until the second defrost period (approximately 9 A.M.), then closed completely. Figure 9a shows a decrease in all temperatures after the shields were closed. The product temperature at the bottom decreased greater than the product temperature at the top. This created a large difference between the two product temperatures.

Conversely, the gap between the mid air curtain temperature (MAT) and the return air temperature (RAT) decreased after the shields were closed. This could have been due to the re-circulation of cold air at the RAT grill, as well as the “stack effect” which pushed the warmer air upwards because of differences in the densities due to the differences in temperatures within the air stream. This caused more of the cold air to enter the RAT grill, thus decreasing the temperature at this location more than at the MAT sensor.

In the second sample day (Figure 9b), the scenario was reversed. The shields were initially closed, and were then opened during the second defrost period. As such, the trends in Figure 9a were reversed in Figure 9b.

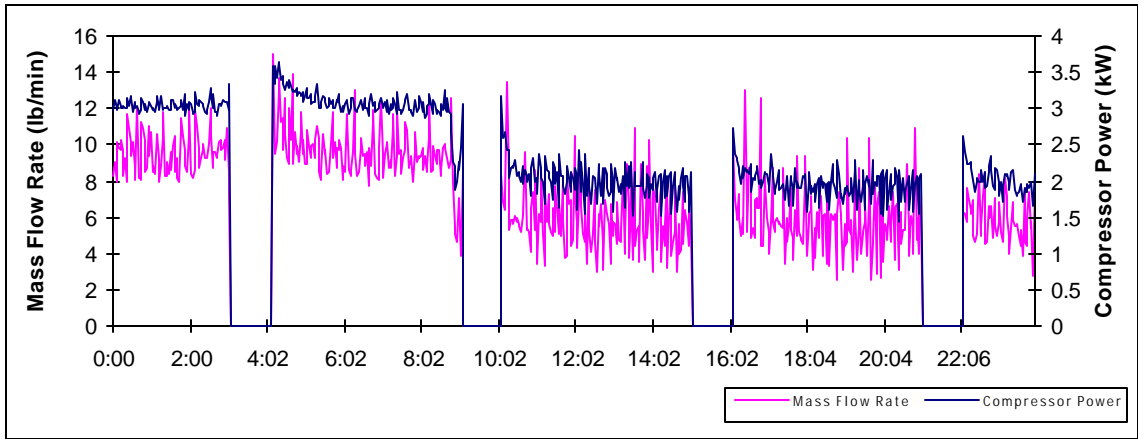


Figure 10a - Mass Flow Rate and Compressor Power Profiles for a sample 24-hour period starting with shields open, then closing them during the second defrost period

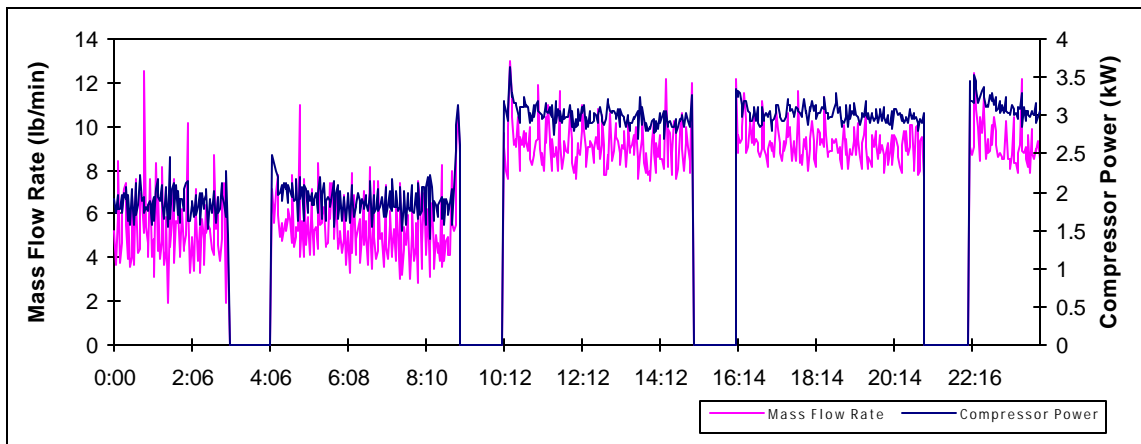


Figure 10b - Mass Flow Rate and Compressor Power Profiles for a sample 24-hour period starting with shields closed, then opening them during the second defrost period

Figures 10a and 10b show the two-minute data points representing the compressor power and mass flow rate profiles for two sample test days. As shown in each Figure, mass flow rate and compressor power drop to zero during all four defrost intervals. During the first day (Figure 10a), the shields were open initially until the second defrost period (approximately 9 A.M.), then closed completely. After the shields were closed, due to a reduction in refrigeration load, the compressor work and mass flow rate decreased. Similarly, when shields were opened after the second daily defrost, mass flow rate and compressor power jumped up to their normal values (Figure 10b).

The second sample day (Figure 10b), the scenario was reversed. The shields were initially closed, and were then opened during the second defrost period. As such, the trends in Figure 10b mirrored those from Figure 10a.

The data points lying above the trend for refrigeration effect and refrigeration load in Figure 11 represent the data for the first hour after the defrost cycle termination. During defrost, the compressor did not provide any cooling. Therefore, the refrigeration load and product temperatures increased, causing an increase in mass flow rate and thus refrigeration effect during the first hour after defrost.

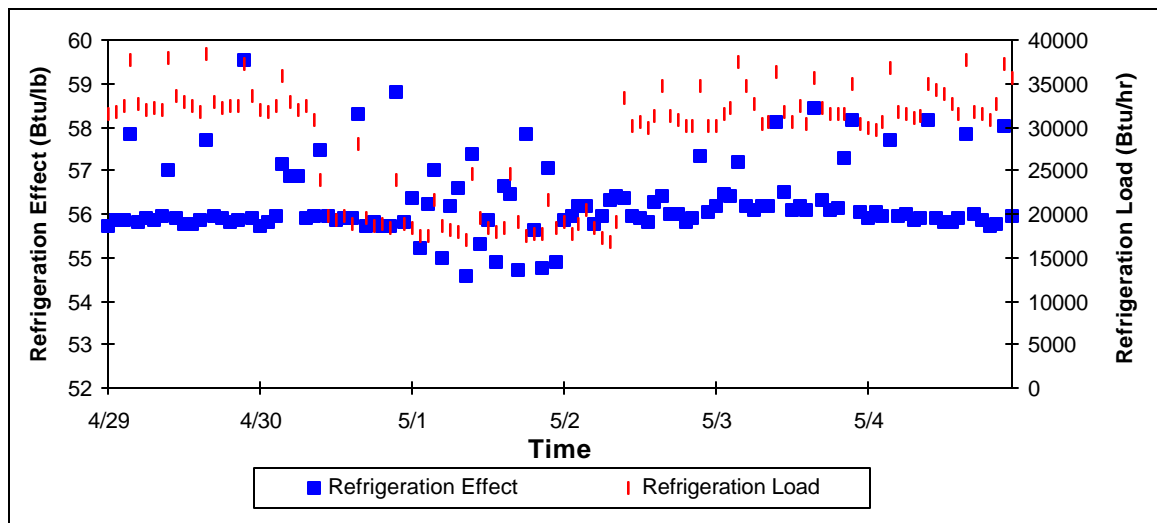


Figure 11 - Refrigeration Effect and Refrigeration Load versus Time  
(No Defrost Data Included)

With the exception of some discontinuity during closing of the shields, refrigeration effect remained fairly constant throughout the test. This relatively non-fluctuating trend was the result of the constant saturated condensing temperature setting and the effect of the evaporator pressure regulator valve on the coil in maintaining steady state temperature. The refrigeration load of the case, on the other hand, fluctuated as the shields were opened and closed (Figure 11). The shields were closed during the second defrost period on April 30<sup>th</sup>. Figure 11 shows a large drop in the refrigeration load at the same time. Likewise, the refrigeration load increased to its original value as the shields were re-opened on May 2<sup>nd</sup>.

Utilizing the shields for an average of 6 hours daily, under the non-24-hour supermarket with shields scenario, resulted in a 1.2 °F decrease in average discharge air temperature over the base case scenario (Figure 12). Similarly, during the holiday scenario, a reduction of 3.4 °F occurred.

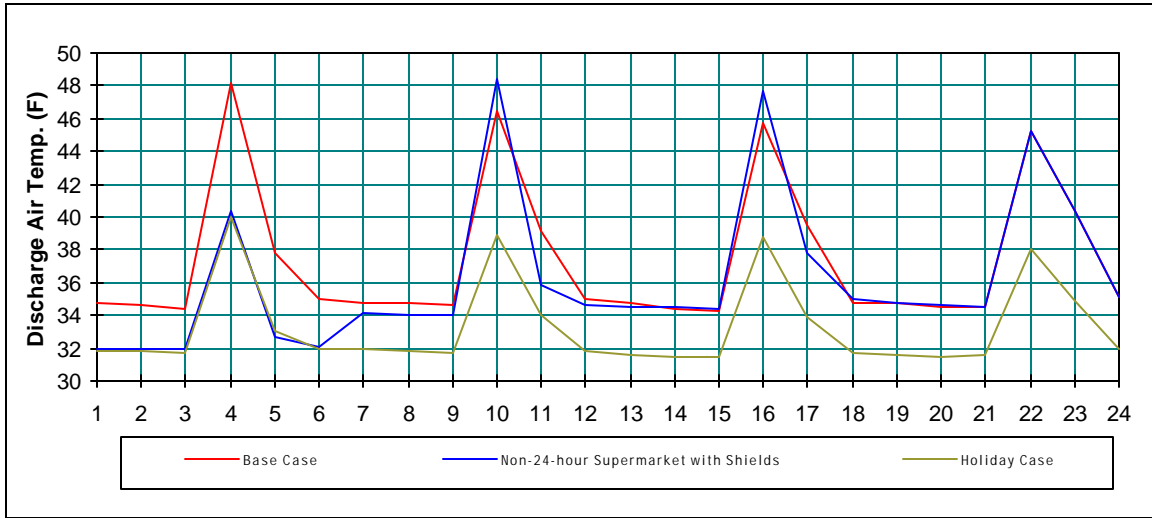


Figure 12 - Average Discharge Air Temperature Comparison Between Base Case, Non-24-hour Supermarket with Shields Case, and Holiday Case

The discharge air temperature increased by as much as 15 °F during defrost which caused the product temperature to increase slightly by approximately 1 °F (Figures 13a and 13b). The product temperature continued to rise until refrigeration was restored and the discharge air temperature dropped below that of the product. While utilizing the shields, the discharge air temperature increased by an even lesser amount during the defrost periods, which in turn produced little change in the product temperature during the majority of the defrost periods.

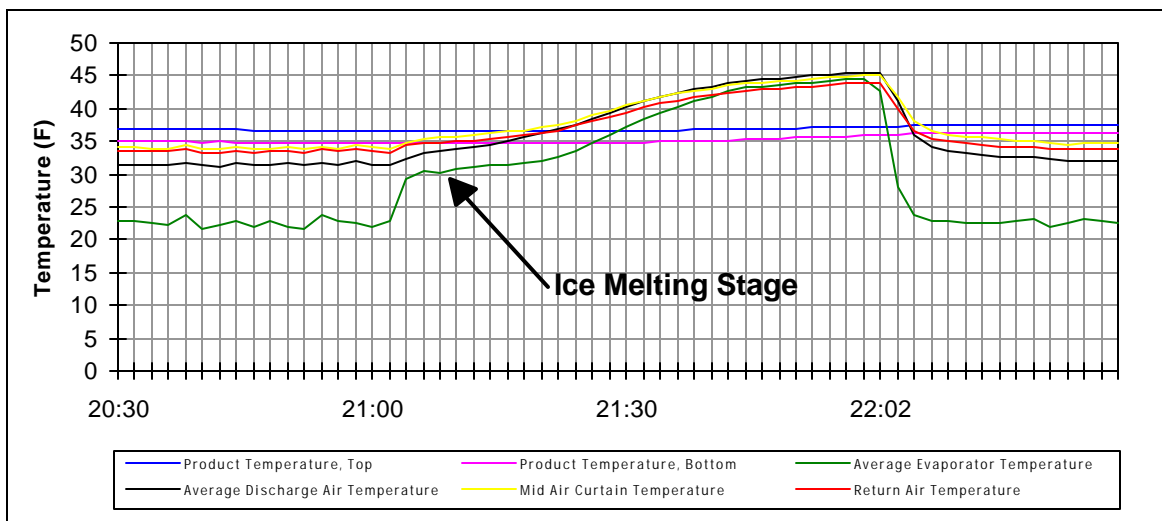


Figure 13a - Last Defrost Period of the Day after Shields were Closed

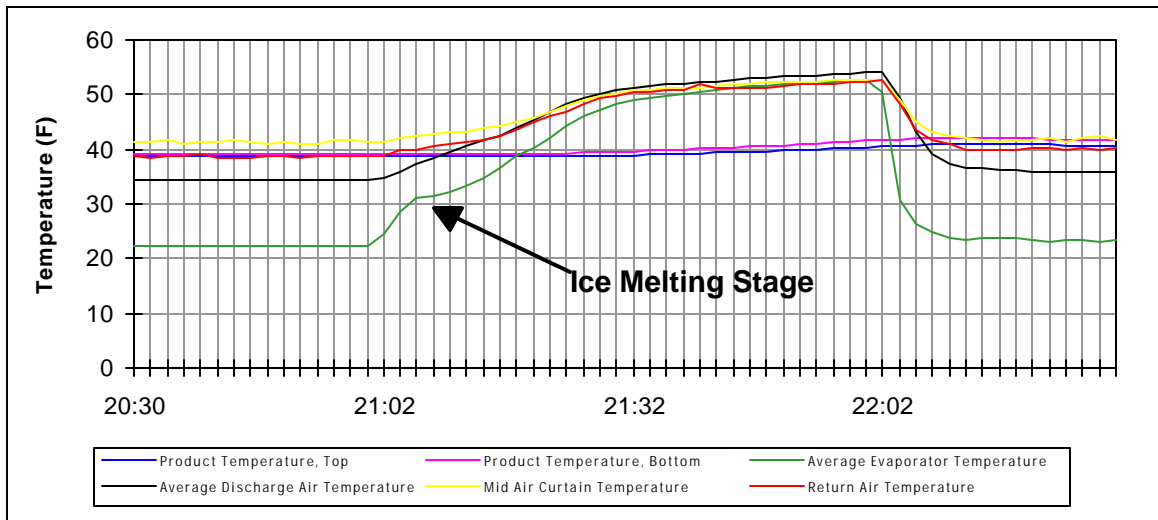


Figure 13b - Last Defrost Period of the Day after Shields were Opened

Another observation from the test was the effect of the shields on the time necessary to defrost the ice on the evaporator coils. Figures 13a and 13b show the time needed to melt the coil ice with and without the shields. The medium temperature display case used in this test utilized an off-cycle defrost to remove ice build-up from the case coil. During off-cycle defrost, the refrigeration to the case was shut down while the case fans continued to run using the ambient air to melt any ice that had built up on the coil.

During defrost, the coil temperature rose from approximately 22.5 °F to 32 °F, at which time, ice started melting. Figures 13a and 13b each point to a region during the middle of the defrost period named the ice melting stage. The evaporator temperature stayed at 32 °F throughout the phase change of ice from solid to liquid state. This ice melting stage was approximately twice as long with the shields closed than with the shields open (12 minutes versus 6 minutes). With the shields closed, less warm ambient air from the room was available to aid melting of the ice on the evaporator coils. The average discharge air temperature was approximately 2 °F cooler with the shields closed than open (Figure 12). The cooler discharge air temperature and the lack of sufficient defrost heat (infiltrating from the room to the case) explains the longer melting time.